Review Article

# Diffusion weighted magnetic resonance imaging and its recent trend—a survey

**Geetha Soujanya Chilla[1], Cher Heng Tan[2], Chenjie Xu[1], Chueh Loo Poh[1]**

[1]School of Chemical & Biomedical Engineering, Nanyang Technological University, Singapore 637459, Singapore; [2]Department of Diagnostic Radiology, Tan Tock Seng Hospital, Singapore 308433, Singapore

*Correspondence to:* Chenjie Xu; Chueh Loo Poh. School of Chemical & Biomedical Engineering, Nanyang Technological University, Singapore 637459, Singapore. Email: cjxu@ntu.edu.sg; CLPoh@ntu.edu.sg.

**Abstract:** Since its inception in 1985, diffusion weighted magnetic resonance imaging has been evolving and is becoming instrumental in diagnosis and investigation of tissue functions in various organs including brain, cartilage, and liver. Even though brain related pathology and/or investigation remains as the main application, diffusion weighted magnetic resonance imaging (DWI) is becoming a standard in oncology and in several other applications. This review article provides a brief introduction of diffusion weighted magnetic resonance imaging, challenges involved and recent advancements.

**Keywords:** Diffusion weighted magnetic resonance imaging (DWI); diffusion weighted MRI (DW-MRI); functional imaging; magnetic resonance imaging; magnetic nanoparticles

Submitted Jan 13, 2015. Accepted for publication Jan 15, 2015.
doi: 10.3978/j.issn.2223-4292.2015.03.01
**View this article at:** http://dx.doi.org/10.3978/j.issn.2223-4292.2015.03.01

## Principles and concepts

Diffusion is the movement of molecules in a system and is one of the transport phenomena, depending on the surrounding environment like temperature, size of molecules, etc. The motion of molecules in any fluid (e.g., water) is random. Since it is difficult to estimate diffusion pattern of individual molecules, diffusion of a group of molecules (e.g., in a voxel) is studied. This diffusion represents the net displacement of that entity of molecules, from time $t_0$ to time $t_1$. In a free medium, molecules can diffuse freely in all directions. This is termed as isotropic diffusion where there is no preferred direction for diffusion. An example is cerebrospinal fluid where diffusion rate of molecules is equal in all directions. In a restricted medium however, the motion of molecules will be limited in the direction of obstruction. In this case, diffusion is anisotropic, which means that the amount of diffusion in not equal in all directions. This directionality largely depends on the cellularity and cell integrity in the tissues (1). An example is diffusion in neural tracts, where water molecules diffuse more in the direction longitudinal to tract than to the sides.

### *Diffusion weighted magnetic resonance imaging (DWI)*

Water forms a large percentage of body weight composition as intra and extra cellular fluids in human body. In biological tissues, diffusion of water molecules follows a pattern according to tissue structure and properties. In some pathological conditions like acute stroke, this diffusion pattern is disturbed and the amount of diffusion changes in affected area. Through studying these changes in diffusion, the abnormalities can be detected. This can be achieved using a specialized magnetic resonance imaging technique called Diffusion Weighted MRI (DW-MRI) or DWI, wherein the diffusion of the water molecules is exploited to visualize internal physiology. The image contrast in DWI reflects the difference in rate of diffusion between tissues. The first quantification of diffusion changes was pioneered by Stejskal and Tanner, in which they made image contrast to be dependent on

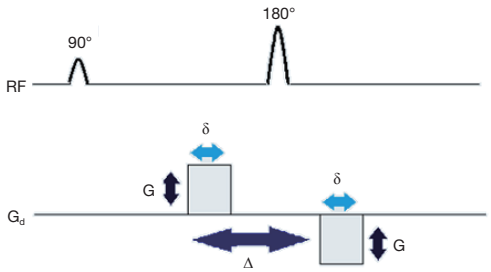


**Figure 1** Diffusion weights addition to MR spin echo sequence. Two gradient pulses (denoted on diffusion gradient line, $G_d$) of amplitude G and duration δ, equal and opposite in effect, are applied in a span of time Δ, symmetric to the 180° radiofrequency pulse (denoted on the line, RF) in a spin echo sequence. After the application of first gradient, protons dephase and on application of second gradient, the uniform phase of protons is regained (rephasing). In case of no net movement of protons in between the two gradient applications, both the gradient effects cancel out each other and there will be no signal attenuation. However, if proton diffuses, there will not be complete rephasing of proton spins and there will be attenuation in signal resulting in darker regions on captured DW images.

diffusion (2). However, it was Le Bihan *et al.* (3), Taylor *et al.* (4), Merboldt *et al.* (5), who implemented DWI first in 1985. Subsequently, Le Bihan *et al.* applied DWI on human brain for the first time in 1986 (6).

To generate diffusion weighting in an MRI image, the readout signal is made dependent on applied diffusion gradients, which can be added to conventional MR sequences like a spin-echo sequence. *Figure 1* depicts diffusion weighting addition to a MRI spin echo sequence. Two diffusion gradients (shown on $G_d$) of magnitude G, one dephasing and one exactly opposite rephasing gradient are added to a MR sequence, symmetric to the 180° RF pulse.

The first gradient introduces phase shift to the protons depending on their positions while the second gradient will reverse the changes made by first gradient. If there are movements of protons, the second gradient will not be able to completely undo the changes induced by the first gradient. As a result, there will be signal attenuation. This signal loss from net movement of particles is given by Stejskal-Tanner equation:

$$S(b) = S_0 e^{-bD} \quad [1]$$

where S(b) refers to the signal received for that particular gradient value (or *b-value* '*b*') and $S_0$ is the signal strength without any diffusion weighting, D is diffusion or 'Apparent Diffusion Coefficient' (*ADC*). The b-value or 'b', is given by the equation

$$b = \gamma^2 G^2 \delta^2 \left( \Delta - \frac{\delta}{3} \right) \quad [2]$$

where γ is the gyromagnetic ratio of hydrogen proton, a constant, given as 42.58 MHz/T, G is the magnitude of applied gradient, δ is the duration of gradient and Δ is the time between the application of the two gradients. From equations 1 and 2, it is evident that the signal loss is dependent on time between pulses, strength and duration of gradients applied. Through this signal dependency on particle motion, DWI is able to generate image contrast through exploiting the diffusion property of water molecules in tissues. For detailed physics and mechanics of diffusion and DWI, readers can refer to (1).

Clinically, several DW images can be obtained by altering the applied gradients' strength and magnitude (b-value), which are referred as DW images at particular b-value. At higher b-values, the effect of diffusion is more pronounced in the images (7) and tissues with high diffusion are seen as hypo-intense regions in the image while tissues with restricted diffusion are seen as hyper-intense regions. *Figure 2* shows three example prostate DW images obtained at b-values 0, 50 and 1,000. The DW image at b-value 0 is obtained without gradient application (b=0) and hence does not carry diffusion information. *Figure 2B,C* are DW images with increasing diffusion weighting.

Since the DWI sequence is a modified MR sequence, all DW images have T1 and T2 contrast in addition to the intended diffusion contrast. Therefore, sometimes, even though there is hyper-intense signal on DW image, it might be due to high T2 signal (T2 shine-through effect) rather than restricted diffusion (e.g., in the case of sub-acute stroke). To avoid these effects, complete diffusion maps called ADC maps are derived from at least two DW images using the Stejskal-Tanner equation. ADC value at any given voxel is calculated as the slope of the log of the signal intensity ratios of the corresponding voxels in two images versus the net b-value graph.

$$ADC \cong \left[ \ln \frac{S(b_2)}{S(b_1)} \right] \bullet \frac{1}{b_1 - b_2} \quad [3]$$

In addition to eliminating T1 and T2 contrast effect in the images, ADC maps also help in quantifying diffusion. Further, the diffusion changes inside the tissue and the signal intensity on ADC map are directly related—if diffusion is lower in the tissue, it shows as a hypo-intense

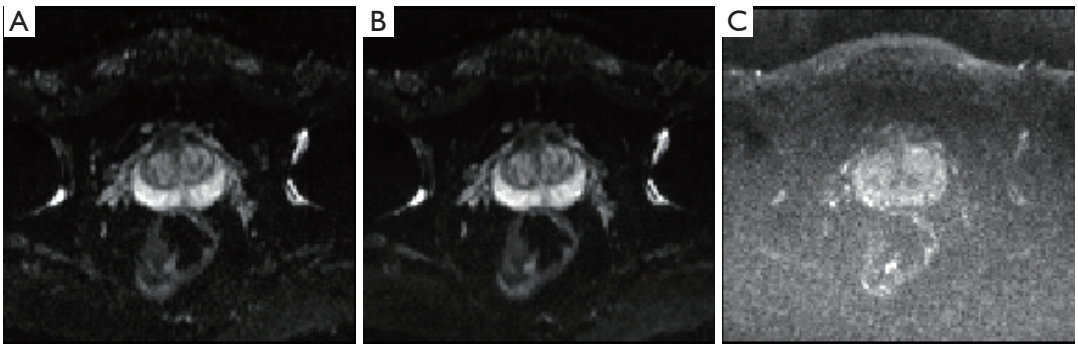


**Figure 2** Diffusion weighted images of prostate obtained at (A) b-value 0, (B) b-value of 50 and (C) b-value of 1,000. All images are taken in transversal plane.

area on ADC maps and if diffusion is higher, it is shown as hyper-intense region on the map.

### *Advantages of adding DWI to conventional MRI sequences*

DWI is particularly useful in several cases, where conventional MR sequences like T2 weighted imaging (T2WI) do not show significant changes in the images. For instance, in pathological conditions like stroke arising from ischemia, signal intensity on T2WI does not change until at least 8 h after the onset of stroke and then appears hyper-intense in the stroke region. However, DWI and ADC maps can show the changes in brain as early as 30 min or even earlier, after the onset of stroke (8,9). The signal intensity changes over time in DWI and ADC maps, changing from hyper-intense signal to hypo-intense signal on DW images and from hypo-intense to hyper-intense signal on ADC maps, from acute to chronic stage (9,10). Pathological changes like these can be detected in its early stages using diffusion images of DWI, even when other modes of imaging might not show significant changes in tissue.

Typically, diffusion is restricted in solid tumors. While conventional MR sequences like T2WI can detect most of the tumors, employing only these conventional sequences would limit the diagnosis due to false positive findings that are commonly present, such as benign prostatic hyperplasia, hemorrhage, hormonal therapy and concomitant prostatitis. Employing DW images and ADC maps, which show hyper-intense signal and hypo-intense signal in tumor regions respectively, would limit false positive diagnosis. However, the conventional MR sequences cannot be completely replaced by DWI alone because of the lower image quality (resolution, noise, blur, etc.) and artifacts present in the DW images. In addition, sequences like T2WI provide anatomical information, which DW imaging cannot provide since it concerns more with diffusion related changes in the tissue. Hence, DWI is suitable to complement the conventional MR sequences by providing diffusional information, to increase the clinical confidence and reduce false positives arising from using only one imaging technique.

In ischemia, DW images clearly show superiority in identifying stroke onset area, even when conventional MR sequences couldn't show any significant changes. Lansberg *et al*. (11) concluded that the addition of DWI improves the accuracy of stroke region identification in the first 48 h after onset of stroke. Kinner *et al*. (12) showed a 10% improvement in diagnostic confidence by the addition of DW images to T2 weighted and contrast enhanced T1 weighted images for the detection of lesions in bowel MRI. Haradome *et al*. (13) studied the value addition of DWI for discriminating malignant and benign focal liver lesions and concluded that the combination of T2 weighted and DWI improves diagnostic confidence. Similar conclusion was drawn by Le Moigne *et al*. (14) for characterizing small hepatocellular carcinoma in case of cirrhotic liver and Fruehwald-Pallamar (15), in identifying false positive lesions in liver. Nishie *et al*. (16) concluded that the combination of super-paramagnetic iron oxide (SPIO)-enhanced MRI and DWI improved the detection of hepatocellular carcinoma in comparison to SPIO alone. Finally, Haider *et al*. (17) concluded that combination of T2 and DW MRI is better in detection and localization of prostate cancer than using T2 MRI alone. Therefore, employing DWI with conventional MR imaging improves diagnostic confidence.

 

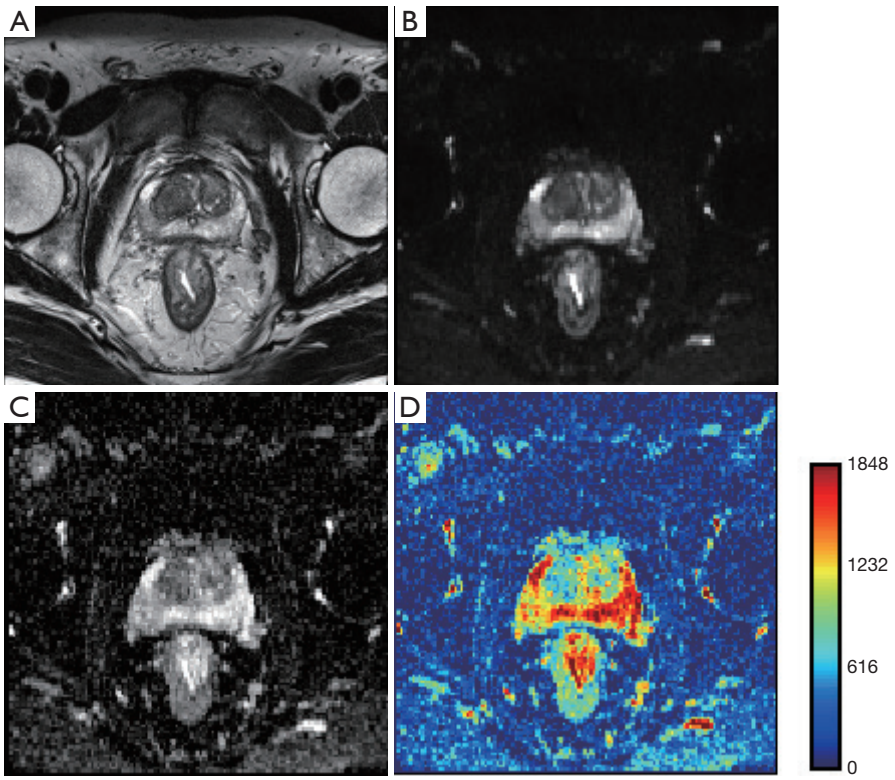


**Figure 3** Illustration of a (A) T2 weighted image, (B) DW image of b-value 50, (C) ADC map in grayscale and in (D) color map. The ADC maps are derived from DW images of b-values 50 and 1,000, in a prostate cancer patient. Left apex, Mid-pole and base are confirmed to be malignant through the multi-modality protocol approach and subsequent TRUS Biopsy. ADC, Apparent Diffusion Coefficient.

Since DWI has the advantage of being acquired very rapidly without specialized hardware, it can be performed in the same sitting along with conventional MR sequences. A basic sequence can be completed in 1.5 to 3 min and may be interpreted either visually (as greyscale imaging) or quantitatively (as a function of diffusivity, i.e., ADC). *Figure 3* shows T2WI and DWI scan images of a prostate cancer patient. *Figure 3B* is diffusion weighted image and *Figure 3C,D* are corresponding ADC maps shown in greyscale and in color map.

## Clinical significance

Even though DWI is widely used for brain related applications now, it was initially applied to distinguish liver tumors from angiomas by Denis Le Bihan as stated in (1). However, it was not an successful attempt because of the presence of large amount of respiratory motion related artifacts and hence, the application was soon switched to human brain (6). Since then, human brain study has been the major domain of application with several studies establishing the potential of DWI in early detection of ischemic stroke (18-23), discriminating brain tumors (24-26), tracking of fibers, etc.

### *DWI for brain imaging*

DWI is currently a standard in diagnosis of ischemic stroke since diffusion changes can be seen early in DW images and ADC maps (9,19,27). In addition to stroke, DWI is also used in diagnosis of epilepsy and neurotoxicity (28,29).

Fiber tracking or tractography was achieved through Diffusion Tensor Imaging (DTI) (30-33), which branched off from DWI. DTI relies on estimating diffusion tensors, which can be obtained through taking DW images in multiple directions. In white matter of brain, diffusion is assumed to be highest, parallel to the tract and studying this anisotropic diffusion would enable us in mapping white matter pathways (white matter tractography). Through DTI of gray matter, connectivity in brain could be

 

understood better. Studying white matter and gray matter in brain, not only helps advance our knowledge on anatomy of brain (34-39) but also allows the diagnosis of white matter and gray matter related pathologies like lesions, axonal injuries, demyelination, multiple sclerosis (40,41), psychiatric disorders like Schizophrenia, ADHD (42-44) and neurological and neuro-degenerative disorders like cognitive impairment, Alzheimers' disease etc. (45,46). Currently, tractography is also used in parcellation and connectivity mapping in brain, in the Human Connectome Project, which aims at mapping the brain at regional level (47,48).

### *DWI for cancer diagnosis*

Another major application of DWI is in oncology. Currently DWI plays an important role in diagnosis and treatment of cancer. Even though the initial attempt of utilizing DWI in liver to discriminate tumors from angiomas was not successful, Yamada *et al*. (49) first showed that employing DWI could be beneficial in discriminating hepatic lesions in 1999. Since then effort has been done to extend DWI to oncological applications involving other organs. As a result, DWI has been increasingly incorporated in routine clinical imaging as an adjunct MRI technique and has shown great promise for tumor detection, staging, monitoring and predicting treatment response in various organs (50,51).

In oncological diagnosis, DW images and ADC maps are combined with conventional MR sequences (e.g., T2WI) for diagnosis. In the diagnosis of cancers like localized prostate cancer, conventional MRI evaluation utilizes high resolution fast spin echo MRI (T2WI) to provide visualization of the structure (prostate gland) and surrounding structures and DWI, to improve lesion detection and localization. Lim *et al*. (52) showed that combining T2WI and DWI imaging significantly increased the area under the receiver operating characteristics curve (AUROC) among readers from 0.66-0.79 for T2WI to 0.76-0.9 for combined DWI and T2WI ($P<0.001$) in prostate cancer.

DW images and ADC maps are also employed for characterizing the lesions as either benign or malignant, using ADC values. Malignant tumors usually have lower ADC values than the ADC of benign tumors, which can help in differentiating between the two (53). During cancer treatment, DWI can also be used to determine the effectiveness of cancer treatment, where cell death and subsequent necrosis (decreased diffusion) can be indicators (54,55). Therefore, DWI is also useful in estimating treatment response in radiotherapy and chemotherapy.

DWI been used in many applications in oncology for a wide range of tissues including prostate (56-58), breast (59), liver (60), kidneys (61), musculoskeletal system (62), liver (51) and is also being employed in whole-body imaging as well (DWIBS—Diffusion-weighted whole-body imaging with background body signal suppression) (54). A recent study by Ai *et al*. (63) employed DWI with DCE-MRI in the diagnosis of benign and malignant tumors in tongue.

### *DWI for other applications*

Apart from brain tractography, DTI can also provide information which could direct towards the integrity of muscle and nerve fibers, aiding in the diagnosis of muscle related injuries or abnormalities. DTI has been employed in studying nerve plexus (64-69) and muscle fibers including skeletal muscles (70). These studies include applications in tongue, thigh and leg muscles, pelvis, spinal cord as well as optical and peripheral nerve related injuries (71-79).

## Challenges with DWI

In current clinical settings, most of the MR scanners operate at 1.5T or 3T. The gradient coils can generate gradient magnitudes around 40 $mTm^{-1}$ and can switch up to a rate of 200 $Tm^{-1}{\cdot}s^{-1}$ (80), and would enable DW measurements up to b-values, approximately of order 1,000 (81). So far, Echo Planar Imaging (EPI) sequences like Single-Shot EPI (SS-EPI) that enable faster image acquisition in short time, typically 20-100 ms are being used clinically. On a 3T scanner, SS-EPI can achieve a DW image with acquisition matrix of 128 × 128 and an isotropic resolution limited to 2 mm. In anisotropic scans, in-plane resolution can be improved to 1 mm, but at a lower Signal-to-Noise Ratio (SNR) (82).

The physics behind diffusion image acquisition assumes perfect field homogeneity, infinitely fast gradient changes, perfectly shaped RF pulses, etc. However, in reality, this is impossible because of power requirements, hardware limitations and other external factors, which limit DWI accuracy and result in lower image quality and other artifacts in the image. Due to its requirements like the need for faster acquisition, very strong gradients, perfect field homogeneity etc., which are not feasible with the existing hardware, the images acquired from DWI fall short of other MR images like T2WI in terms of image quality, like distortion, noise, low resolution, and limited morphological interpretability.

 

### *Resolution, SNR and contrast*

DW images are usually of lower resolution than conventional MR images like T2WI. This is due to multiple factors like low strength scanners, faster image acquisition techniques like Single-Shot Echo Planar Imaging and limitations of general acquisition parameters like field of view (FOV), slice thickness, etc. Lower strength scanners contribute weaker signals to the image compared to high strength scanners and thereby provide lower resolution than the low strength scanners. Fast acquisition techniques like SS-EPI concentrate on acquiring images in a very short time before complete signal decay and therefore have limitations on the maximum achievable resolution of DW images. General MR acquisition parameters like FOV, slice thickness, matrix size etc. are also related to spatial resolution. Increasing FOV but maintaining same matrix size would decrease resolution of image (in-plane spatial resolution of an image can be calculated by dividing FOV with matrix size) and increasing the matrix size would increase the in-plane resolution if FOV remains constant. In general, the resolution along the slice direction (through-plane) is poorer compared to direction of image (in-plane). However, the maximum resolution achievable by optimizing these parameters is limited by the hardware limitations of scanner. Low resolution can be a challenge in radiotherapy planning treatment since DW images, along with ADC maps are used in conjunction with T2-weighted images, which typically are of higher resolution. Given the difference in the respective resolutions, if ADC and T2WI were to be super-imposed, due to the low resolution of ADC/DWI, it would over estimate lesion area due to its lower resolution. And in general, higher resolution images are preferred since they offer more data and accurate details compared to lower resolution images.

In addition to low resolution, DW images also suffer from low SNR, because of the presence of large amount of noise. Image contrast is also a crucial issue since higher contrast is very beneficial in delineating the regions of abnormality accurately using diffusion coefficient values from ADC maps. Lower SNR and contrast-to-noise-ratio (CNR) can limit the ability of accurate interpretation of ADC maps and DW images.

### *Artifacts*

DW images are often susceptible to various artifacts like distortion, ringing etc. which arise from a multitude of factors. One of the most important artifacts in DW images is distortion. Distortion in images can occur due to field inhomogeneity and differences in magnetic susceptibility in the region being imaged.

Widely used 3T scanners were introduced in early 2000s and were adapted quickly due to their ability to achieve increased spatial resolution, higher SNR and better contrast than 1.5T machines. However, increasing field strength contributed to higher magnetic susceptibility related artifacts in the image. The B1 magnetic field, in which the patient is placed, becomes more inhomogeneous as field strength increases, contributing to more errors in image acquisition (83). Sequences like EPI require very homogeneous magnetic fields so that the proton spins conform to the spin rate and do not dephase, ensuring accuracy in imaging. However in several cases, like at air-tissue interfaces for instance, protons at the interface undergo phase change different from the expected due to magnetic susceptibility differences thereby causing geometric distortion in the image. *Figure 4A* shows a T2 weighted image and *Figure 4B* shows the corresponding DW image of a phantom. The phantom is placed in air and scanned due to which distortion occurred around the edges with air-interfacing in the DW image, *Figure 4B*.

This distortion can also be observed when imaging is done in tissues with metal implants, due to field variation in the region. This susceptibility related artifacts can also be caused by the gradient system, which could introduce inhomogeneity in magnetic field. Powerful and rapidly switching gradients induce local currents called eddy currents, which in turn produce local magnetic fields of their own, disturbing the field homogeneity. These eddy currents contribute to distortion and image shift, by manipulating the gradient strengths experienced by spins (84), which affect accurate image interpretation and ADC estimation and thereby, clinical diagnosis. Eddy currents can also cause other artifacts such as ghosting (84).

Apart from distortion, EPI sequences are sensitive to motion, microscopic or macroscopic, arising from various factors. Macroscopic motion leads to severe motion related artifacts resulting in ghosting or blurring of the DW image. For DW imaging, this could affect diffusion measurements greatly and might render incorrect data in the image (2,85). Even though precautions can be taken to minimize voluntary patient movement, involuntary movements like breathing, blood flow or mechanical vibrations arising from patient table of the scanner are still unavoidable.

 

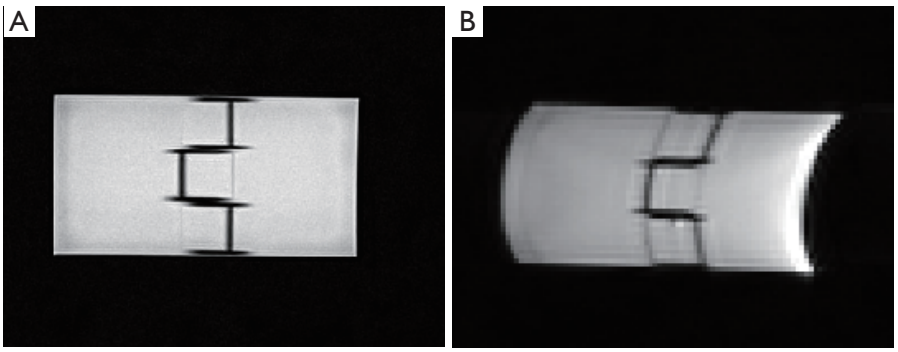


**Figure 4** Illustration of a (A) T2 weighted image (scanned resolution: 0.4×0.4 $mm^2$) and (B) a distorted DW image of b-value 50 (scanned resolution: 1.4×1.4 $mm^2$) of a rectangular phantom. The phantom had air interface during scanning and the resulting distortion can be seen in DW image *Figure 4B*.

### *Other*

Currently most of the ADC measurements rely on acquiring at least two DW images and deriving ADC maps using Stejskal-tanner equation. However, this holds true only when the diffusion inside tissue is mono-exponential, which might not be the case always as there have been some studies which deduced that diffusion in some tissues is more accurately characterized by a bi-exponential model or multi-exponential model (86) and in cases like these, deriving ADC maps through mono-exponential model would not accurately estimate diffusion in tissues.

## Technological advancement in addressing the challenges

DW images often have lower image quality compared to other conventional MR images due to image quality issues like distortion, noise, low resolution and presence of artifacts, most of which arise due to the usage of faster image acquisition techniques such as EPI, essential for capturing the diffusion signal before it becomes null.

Most of these challenges can be circumvented by altering DW-MR protocol factors like echo time (TE), gradient strengths, changing image acquisition techniques etc. Broadly, the approaches to counter the inherent challenges associated with DWI fall into four categories: hardware upgrading or improvements, usage of contrast agents, optimizing acquisition parameters, and software based post-processing techniques (*Table 1*). None of these approaches fully address all the challenges individually, as these might come with their own challenges like increased acquisition time, etc. This section deals with these four categories of approaches, challenges they minimize and any other challenges they might bring in. Choice of opting for an approach in addressing issues therefore, is dependent on its limitations as well as other considerations like patient safety, cost, value addition, accuracy, etc.

### *Hardware improvements*

Effectiveness of diffusion imaging largely depends on the ability of hardware in mimicking ideal behavior as well as on the imaging parameters. Though ideal behavior from hardware is expected even in conventional MR imaging, T1 and T2 imaging is relatively stable to the deviations from this ideal behavior compared to DWI. This deviation can limit DWI accuracy and result in image artifacts. However, approaches involving hardware upgrade or improvements could be beneficial in tackling some the challenges involved in DW imaging.

#### Increasing field strength

Employing higher strength MR scanners provides much better contrast, resolution and SNR, in DW imaging. This also reduces the acquisition time in case of DTI. A study by Polders *et al*. (87) assessed DTI at 1.5T, 3T and 7T and showed an increase in SNR and reduction in the uncertainty in DTI estimates with 7T scanners. At the current clinical scanner strengths, low resolution DW images are preferred, to ensure good SNR, at the cost of finer details in the image (85) since increasing resolution would mean reduction in SNR. Therefore, employing ultra-high field scanner like 7T scanners could improve spatial resolution without sacrificing SNR, enabling better diagnosis (88). However, at higher fields, the T2 and T2*

 

**Table 1** Challenges of DWI and some approaches to address these challenges

| Challenge | Some common approaches to address challenges |
|---|---|
| Low resolution | Hardware improvements |
| | Increasing field strength of scanners |
| | Multi-shot sequences |
| | Post-processing |
| | Interpolation techniques; super-resolution reconstruction |
| SNR | Hardware improvements |
| | Increasing field strength of scanners; High strength gradients |
| | Multi-shot sequences |
| | Acquisition parameters |
| | Averaging |
| Contrast | Contrast agents |
| Acquisition time | Hardware improvements |
| | Increasing field strength of scanners; high strength gradients |
| | Single-shot sequences |
| | Parallel imaging |
| | Acquisition parameters |
| | Optimal TR, TE, number of b-values |
| Distortion from susceptibility differences and eddy currents | Hardware improvements |
| | Increasing field strength of scanners; high strength gradients; shimming coils |
| | Non-EPI based sequences |
| | Calibration scans and pre-emphasized pulses |
| | Acquisition parameters |
| | Increasing receiver bandwidth or decreasing peak gradient amplitudes |
| | Post-processing |
| | Acquiring field maps and correction algorithms |
| Motion artifacts | Hardware improvements |
| | Single-shot EPI; Non-EPI based sequences; |
| | Cardiac and Respiratory triggering or bi-polar gradient pulses<br>Navigator based and readout-segmented acquisition methods |
| | Acquisition parameters |
| | Averaging |
| ADC accuracy | Acquisition parameters |
| | Optimal number of b-values |
| | Diffusion modeling in tissue |
| | Post-processing |
| | Acquiring field maps and correction algorithms |

DWI, diffusion weighted magnetic resonance imaging; SNR, Signal-to-Noise Ratio; EPI, Echo Planar Imaging; ADC, Apparent Diffusion Coefficient.

 

relaxation times are reduced and B0 inhomogeneity is increased causing blurring and distortion in the images.

**Powerful gradients and hardware appendages**

The gradients used in DWI determine the signal strength which will be used in the reconstruction of image. Therefore, these gradients must be highly stable and powerful, i.e., they should be able to provide homogeneous field and also be able to switch the field very rapidly. The strong external static magnetic field B0, which is used for magnetization of protons, must be extremely homogenous. This ensures that the proton spins conform to the spin rate and do not dephase, ensuring accuracy in imaging. In addition to B0 homogeneity, RF pulse field, also called B1 field, should also be extremely homogeneous. This is to ensure proper energy transfer from RF pulses (from transmitting coils) to the patient and from the patient to the readout coils (receiver coils). Gradients, which can switch very rapidly, can minimize eddy currents and thereby related artifacts, lower acquisition time, ensure good SNR and minimize susceptibility related artifacts (89). However, as the strength of gradients increases, eddy currents may increase and also vibrations may introduce motion artifacts. To minimize eddy currents in the system, shimming coils can be used. These shimming coils shield the gradients and minimize unnecessary fields outside desired area and thereby stray fields.

To minimize the effect of motion in diffusion imaging, one can opt for hardware based approaches like respiratory triggering, cardiac triggering etc. to minimize effect of motion in the images. Cardiac motion effect can be minimized by employing cardiac triggering at a cost of increased scan time (90,91). Respiratory triggering can be employed to acquire DW images in the same respiratory phase, which can be averaged to get a high SNR image. However, respiratory triggering increases scan time and might have an adverse effect on the reproducibility of ADC values (92,93).

**Imaging sequences and parallel imaging**

In addition to hardware upgrades, the sequence pulses being employed for DWI have a major role in image quality. Typically the sequence pulses chosen for DW imaging should be capable of acquiring diffusion signal before its complete signal attenuation. Since this attenuation happens very fast in the case of diffusing protons, the sequences employed would be able to generate image in a very short time. In addition, they should be able to avoid phase accumulation errors and other artifacts and enable faster acquisition of multiple diffusion images in minimal time, especially for DTI.

The popular sequence employed for DWI is single shot EPI. These SS-EPI sequences are popular due to its ease and shorter image acquisition time, which minimize motion artifacts in the image. However, images obtained through SS-EPI have low SNR and resolution and are prone to EPI related artifacts like nyquist ghosting and chemical shift artifacts. To overcome the challenges posed by SS-EPI, multi-shot EPI sequences have been developed. Typically used for higher resolution scans, multi-shot EPI sequences have been gaining momentum and offer excellent SNR compared to single-shot sequences. The drawback of multi-shot EPI however is the increased acquisition time, typically few seconds (57) and its susceptibility to motion artifacts, especially inter-shot phase inconsistencies. Motion artifacts have been successfully minimized using navigator based acquisition methods which were extended to DWI. A recent navigator based, readout-segmented, multi-shot EPI called RESOLVE is a promising technique, allowing higher resolution and reduced susceptibility and motion related artifacts (94,95).

Parallel imaging is one another strategy employed to reduce the scan times and susceptibility and eddy currents related blurring and distortions. In parallel imaging, redundant acquisition is minimized by acquiring only needed lines in k-space. Parallel imaging techniques like GRAPPA (96) and SENSE (97) can be merged with either single-shot or multi-shot EPI (98). Recent developments in DWI have enabled acquiring 1 mm isotropic resolution at 7T by using a technique called ZOOPPA, which combines zoomed imaging with parallel imaging (51). The drawback of employing parallel imaging however is that there will be loss in SNR.

Non-EPI based pulses can also be employed for diffusion imaging, though not as popular as echo planar sequences. These can either be single-shot or multi-shot sequences like line scan imaging, radial imaging, steady-state free precession diffusion imaging methods instead of single or multi-shot EPI (84,99) and these are much more robust to susceptibility differences. However, some of the drawbacks of these methods are increased acquisition time, motion sensitivity, introduction of phase errors and other artifacts.

To minimize eddy currents effect, using calibration scans (100) or using modified EPI pulses with pre-emphasized pulses (101,102) have also been suggested in the literature. Employing bipolar gradients can effectively minimize motion, eddy currents and ghosting artifacts, even though at an increased acquisition time (103).

 

However, hardware upgrades and sequence alterations are not always feasible, considering the cost factor and limited relevancy for other applications of MRI.

### *Optimizing acquisition parameters*

Acquisition parameters largely influence the image quality and optimizing these parameters can give minimize artifacts and improve image quality. One of the main problems with DWI is the effect of eddy currents, which contributes to distortion and image shift, by manipulating the gradient strengths experienced by spins (84), affecting image interpretation accuracy and ADC estimation. The effects of eddy currents effect can be reduced through increasing receiver bandwidth or by decreasing peak gradient amplitudes (104).

Averaging is one of the most commonly employed techniques, which minimizes the effect of motion on images and increases SNR. In this approach, multiple images are acquired and averaged to reduce the effect of noise and microscopic motion. While averaging is the easiest way to increase SNR compared to hardware upgrades, this increases acquisition time. A common practice to ensure good SNR yet not increase acquisition time is to employ parallel imaging with multiple averages.

Another area where optimizing acquisition parameters like repetition time (TR), TE, choice and the number of b-value measurements etc. could be beneficial in DWI is estimation of ADC. ADC is typically calculated from at least two images. However, more number of b-value DW measurements help in accurate determination of ADC value. Otherwise, two optimal b-value DW images, whose difference is given by 1/D (105), could provide good estimation for ADC within least amount of time irrespective of imaging conditions. It will be a trade-off between better image quality and acquisition time in most of the cases, which should be considered when optimizing. For accurate estimation of ADC, it is also important to know the diffusion profile of water inside the imaging tissue. Diffusion in a tissue largely depends on its structure and properties and since diffusion pattern might differ from one tissue to another (having multi-exponential diffusion profile in the tissue, for instance), ADC calculation must be done considering this into account.

### *Contrast agents*

DW images often suffer with poor interpretability given its limited spatial resolution, limited morphological information and the presence of artifacts. An approach to increase image contrast is to use magnetic nanoparticle contrast agents with DWI, called magnetic nanoparticles (MNPs)-enhanced MRI. Magnetite ($Fe_3O_4$) NPs or MNPs, are made in sizes smaller than 20 nm in diameter whose magnetization directions are subject to thermal fluctuation at room temperature (106). Without external magnetic field, their net magnetization is zero because the fluctuation in magnetization direction minimizes the magnetic interactions between NPs. This makes the dispersion stable in solutions and facilitates NP coupling with biological agents. When being exposed to external magnetic field, however, they align along the field direction, achieving magnetic saturation at a very high magnitude, greater than that of any of the known biological entities. This unique magnetic property has allowed their detectability by T2 and T2*-weighted MRI. In addition, similar to other nano-sized particles, MNPs have a large surface-to-volume ratio, providing abundant chemically active sites for biomolecule conjugation. This property can be used to target specific tissues.

Thoeny *et al*. combined MNP-enhanced MRI and DW-MRI (USPIO–DW-MRI) to detect pelvic lymph node metastases in normal-sized nodes of bladder and prostate cancer patients (107,108). In this study, dextran coated ultra-small super-paramagnetic particles of iron oxide (USPIO) were intravenously injected, transported through vascular endothelium into the interstitial space and subsequently to lymph nodes where particles were taken up by macrophages. The accumulation of USPIO led to the signal decrease on T2 and T2*-weighted MR images. However, in metastatic lymph nodes, tumor cells replace normal tissue and macrophages. Thus the take-up of USPIO is decreased, which do not change the signal intensity in T2 and T2*-weighted MR images (109). Through two consecutive clinical studies [21 patients and 256 patients (107,108)], diagnostic accuracy (90% per patient) was comparable for the classic histopathology and the USPIO–DW-MRI method, while time of analysis with 80 min for the histopathology and 13 min for the USPIO–DW-MRI method was much shorter. Histopathological analysis showed metastasis in 26 of the 802 analyzed nodes (3.2%), of which 92% (24 nodes) were correctly diagnosed as positive on USPIO–DW-MRI.

### *Software post-processing*

To increase image quality and reduce artifacts, post-processing techniques can be employed. The common outcome of magnetic susceptibility differences is geometric

 

distortion in DW images, which is especially severe at the air-tissue interfaces. Due to the nature of EPI sequences, magnetic susceptibility distortions introduce pixel shift. This shift can be corrected by acquiring field maps (110) and employing post-processing techniques, to certain extent.

To increase the spatial resolution of DW images, various image processing techniques have also been used to increase resolution. Traditional interpolation techniques rely on interpolating a high resolution voxel from various low resolution voxels, using finite size kernels like linear, cubic, quadratic, B-Spline, nearest neighbor, Gaussian etc. Some of the newer interpolation methods rely on adaptive methods, which take image features into consideration and utilize it for interpolation. These adaptive methods are computationally much more expensive than non-adaptive methods (111). Each of these methods has their own advantages and disadvantages and the methods are dependent on the type of the application. Comparison of some of the types of interpolation techniques, their performance and comparison can be found in (112,113). Classical interpolation techniques are inherently limited as they do not add any extra information or recover lost high frequency components and they also have associated staircase and ringing artifacts in addition to blurring (114). Another approach to increase spatial resolution of DW images is super-resolution reconstruction method. Unlike traditional interpolation methods, most of the super-resolution reconstruction methods rely on adding information to an image from other sources and minimizing the degradation that occurs in imaging process, to generate a high resolution images. Scherrer *et al*. (82) corrected for the distortion and motion alignment in DWI and generated a isotropic high resolution DW image, which could not be generated clinically within a short time. Several others (85,115-118) have also applied super-resolution on DWI and DTI images in brain.

## Discussion and perspective

DWI has become a standard for tractography, diagnosis of brain related pathologies and oncology as well. In recent years, research in oncology has been directed at uncovering potential uses of DWI. This includes improving detection of tumor foci in areas where conventional high resolution fast spin echo MRI has limitations. It is advantageous, for example in cases like prostate cancer, to monitor areas of hemorrhage following TRUS biopsy in the transitional zone and also for extra-prostatic involvement such as urinary bladder and seminal vesicle invasion (119). Preliminary studies have shown potential of DWI for prognostication of disease since diffusivity appears to correlate with tumor grade (differentiation) and tumor burden (120). This might help in non-invasive monitoring of response to treatment and for detection of local tumor recurrence (121).

DWI has come a long way since its inception in mid-1980's and is becoming a standard in many clinical applications. With the advent of faster acquisition techniques and other technological advancements, the gap between current state-of-art imaging and ideal diffusion imaging is reducing. Diffusion measurements are more accurate than before, image resolution has increased and there has been significant reduction in artifacts as well. Powerful gradients, artifact minimizing image acquisition systems and methods are being employed to acquire much more accurate information. Even though hardware upgrades like having higher strength MR machines and image acquisition and reconstruction methods enable much better image quality, these are often expensive. Also, these advances translating into clinical usage is subjected to patient safety and other external factors. Usage of post-processing methods and contrast agents is being employed when possible and viable but there is still need for more research in all these areas to increase the interpretability and quality of DW images. In summary, this paper has discussed some of these issues and solutions addressed in literature so far. Recent advancements look very promising in addressing the challenges involved, which could potentially widen the range of applications where diffusion imaging can be used.

## Acknowledgements

*Funding:* Ms.Chilla is supported by NTU Research Scholarship (MOE). The work is supported by NTU-NHG Innovation Collaboration Grant (ICG/13003 to CLP and CHT) and is partially supported by the Tier-1 Academic Research Funds by Singapore Ministry of Education (RG 64/12 to XCJ) and National Natural Science Funds of China (Grant No. H1819 to XCJ).

*Disclosure:* The authors declare no conflict of interest.

## References

1. Jones DK. Diffusion MRI: Theory, Methods, and Applications. Oxford, USA: Oxford University Press, 2010.
2. Stejskal E, Tanner J. Spin diffusion measurements: spin

 

echoes in the presence of a time-dependent field gradient. J Chem Phys 1965;42:288.
3. Le Bihan D, Breton E. Imagerie de diffusion in-vivo par résonance magnétique nucléaire. C R Acad Sci (Paris) 1985;301:1109-12.
4. Taylor DG, Bushell MC. The spatial mapping of translational diffusion coefficients by the NMR imaging technique. Phys Med Biol 1985;30:345-9.
5. Klaus-Dietmar Merboldt,Wolfgang Hanicke, Jens Frahm. Self-Diffusion NMR Imaging Using Stimulated Echoes. J Magn Reson 1985;64:479-86.
6. Le Bihan D, Breton E, Lallemand D, Grenier P, Cabanis E, Laval-Jeantet M. MR imaging of intravoxel incoherent motions: application to diffusion and perfusion in neurologic disorders. Radiology 1986;161:401-7.
7. Baker S, Kanade T. Limits on super-resolution and how to break them. Pattern Analysis and Machine Intelligence, IEEE Transactions on, 2002;24:1167-83.
8. Srinivasan A, Goyal M, Al Azri F, Lum C. State-of-the-art imaging of acute stroke. Radiographics 2006;26 Suppl 1:S75-95.
9. Allen LM, Hasso AN, Handwerker J, Farid H. Sequence-specific MR imaging findings that are useful in dating ischemic stroke. Radiographics 2012;32:1285-97; discussion 1297-9.
10. van Everdingen KJ, van der Grond J, Kappelle LJ, Ramos LM, Mali WP. Diffusion-weighted magnetic resonance imaging in acute stroke. Stroke 1998;29:1783-90.
11. Lansberg MG, Norbash AM, Marks MP, Tong DC, Moseley ME, Albers GW. Advantages of adding diffusion-weighted magnetic resonance imaging to conventional magnetic resonance imaging for evaluating acute stroke. Arch Neurol 2000;57:1311-6.
12. Kinner S, Blex S, Maderwald S, Forsting M, Gerken G, Lauenstein TC. Addition of diffusion-weighted imaging can improve diagnostic confidence in bowel MRI. Clin Radiol 2014;69:372-7.
13. Haradome H, Grazioli L, Morone M, Gambarini S, Kwee TC, Takahara T, Colagrande S. T2-weighted and diffusion-weighted MRI for discriminating benign from malignant focal liver lesions: diagnostic abilities of single versus combined interpretations. J Magn Reson Imaging 2012;35:1388-96.
14. Le Moigne F, Durieux M, Bancel B, Boublay N, Boussel L, Ducerf C, Berthezène Y, Rode A. Impact of diffusion-weighted MR imaging on the characterization of small hepatocellular carcinoma in the cirrhotic liver. Magn Reson Imaging 2012;30:656-65.
15. Fruehwald-Pallamar J, Bastati-Huber N, Fakhrai N, Jantsch M, Puchner S, Herneth AM, Ba-Ssalamah A. Confident non-invasive diagnosis of pseudolesions of the liver using diffusion-weighted imaging at 3T MRI. Eur J Radiol 2012;81:1353-9.
16. Nishie A, Tajima T, Ishigami K, Ushijima Y, Okamoto D, Hirakawa M, Nishihara Y, Taketomi A, Hatakenaka M, Irie H, Yoshimitsu K, Honda H. Detection of hepatocellular carcinoma (HCC) using super paramagnetic iron oxide (SPIO)-enhanced MRI: Added value of diffusion-weighted imaging (DWI). J Magn Reson Imaging 2010;31:373-82.
17. Haider MA, van der Kwast TH, Tanguay J, Evans AJ, Hashmi AT, Lockwood G, Trachtenberg J. Combined T2-weighted and diffusion-weighted MRI for localization of prostate cancer. AJR Am J Roentgenol 2007;189:323-8.
18. Warach S, Chien D, Li W, Ronthal M, Edelman RR. Fast magnetic resonance diffusion-weighted imaging of acute human stroke. Neurology 1992;42:1717-23.
19. Warach S, Gaa J, Siewert B, Wielopolski P, Edelman RR. Acute human stroke studied by whole brain echo planar diffusion-weighted magnetic resonance imaging. Ann Neurol 1995;37:231-41.
20. Fisher M, Prichard JW, Warach S. New magnetic resonance techniques for acute ischemic stroke. JAMA 1995;274:908-11.
21. Warach S, Dashe JF, Edelman RR. Clinical outcome in ischemic stroke predicted by early diffusion-weighted and perfusion magnetic resonance imaging: a preliminary analysis. J Cereb Blood Flow Metab 1996;16:53-9.
22. Marks MP, de Crespigny A, Lentz D, Enzmann DR, Albers GW, Moseley ME. Acute and chronic stroke: navigated spin-echo diffusion-weighted MR imaging. Radiology 1996;199:403-8.
23. Lutsep HL, Albers GW, DeCrespigny A, Kamat GN, Marks MP, Moseley ME. Clinical utility of diffusion-weighted magnetic resonance imaging in the assessment of ischemic stroke. Ann Neurol 1997;41:574-80.
24. Ebisu T, Tanaka C, Umeda M, Kitamura M, Naruse S, Higuchi T, Ueda S, Sato H. Discrimination of brain abscess from necrotic or cystic tumors by diffusion-weighted echo planar imaging. Magn Reson Imaging 1996;14:1113-6.
25. Sugahara T, Korogi Y, Kochi M, Ikushima I, Shigematu Y, Hirai T, Okuda T, Liang L, Ge Y, Komohara Y, Ushio Y, Takahashi M. Usefulness of diffusion-weighted MRI with echo-planar technique in the evaluation of cellularity in gliomas. J Magn Reson Imaging 1999;9:53-60.
26. Okamoto K, Ito J, Ishikawa K, Sakai K, Tokiguchi S. Diffusion-weighted echo-planar MR imaging in

 

differential diagnosis of brain tumors and tumor-like conditions. Eur Radiol 2000;10:1342-50.
27. Muir KW, Buchan A, von Kummer R, Rother J, Baron JC. Imaging of acute stroke. Lancet Neurol 2006;5:755-68.
28. Balin J, Parmar H, Kujawski L. Conventional and diffusion-weighted MRI findings of methotrexate related sub-acute neurotoxicity. J Neurol Sci 2008;269:169-71.
29. Haykin M, Gorman M, van Hoff J, Fulbright R, Baehring J. Diffusion-weighted MRI correlates of subacute methotrexate-related neurotoxicity. J Neurooncol 2006;76:153-7.
30. Pierpaoli C, Jezzard P, Basser PJ, Barnett A, Di Chiro G. Diffusion tensor MR imaging of the human brain. Radiology 1996;201:637-48.
31. Basser PJ, Pierpaoli C. A simplified method to measure the diffusion tensor from seven MR images. Magn Reson Med 1998;39:928-34.
32. Basser PJ, Pierpaoli C. Microstructural and physiological features of tissues elucidated by quantitative-diffusion-tensor MRI. J Magn Reson B 1996;111:209-19.
33. Basser PJ, Pajevic S, Pierpaoli C, Duda J, Aldroubi A. In vivo fiber tractography using DT-MRI data. Magn Reson Med 2000;44:625-32.
34. Huang H, Zhang J, Wakana S, Zhang W, Ren T, Richards LJ, Yarowsky P, Donohue P, Graham E, van Zijl PC, Mori S. White and gray matter development in human fetal, newborn and pediatric brains. Neuroimage 2006;33:27-38.
35. Pfefferbaum A, Sullivan EV, Hedehus M, Lim KO, Adalsteinsson E, Moseley M. Age-related decline in brain white matter anisotropy measured with spatially corrected echo-planar diffusion tensor imaging. Magn Reson Med 2000;44:259-68.
36. Barnea-Goraly N, Menon V, Eckert M, Tamm L, Bammer R, Karchemskiy A, Dant CC, Reiss AL. White matter development during childhood and adolescence: a cross-sectional diffusion tensor imaging study. Cereb Cortex 2005;15:1848-54.
37. Assaf Y, Pasternak O. Diffusion tensor imaging (DTI)-based white matter mapping in brain research: a review. J Mol Neurosci 2008;34:51-61.
38. Giorgio A, Watkins KE, Chadwick M, James S, Winmill L, Douaud G, De Stefano N, Matthews PM, Smith SM, Johansen-Berg H, James AC. Longitudinal changes in grey and white matter during adolescence. Neuroimage 2010;49:94-103.
39. Hong JH, Son SM, Jang SH. Identification of spinothalamic tract and its related thalamocortical fibers in human brain. Neurosci Lett 2010;468:102-5.
40. Rovaris M, Gass A, Bammer R, Hickman SJ, Ciccarelli O, Miller DH, Filippi M. Diffusion MRI in multiple sclerosis. Neurology 2005;65:1526-32.
41. Inglese M, Bester M. Diffusion imaging in multiple sclerosis: research and clinical implications. NMR Biomed 2010;23:865-72.
42. Peters BD, Blaas J, de Haan L. Diffusion tensor imaging in the early phase of schizophrenia: what have we learned? J Psychiatr Res 2010;44:993-1004.
43. Kubicki M, McCarley R, Westin CF, Park HJ, Maier S, Kikinis R, Jolesz FA, Shenton ME. A review of diffusion tensor imaging studies in schizophrenia. J Psychiatr Res 2007;41:15-30.
44. van Ewijk H, Heslenfeld DJ, Zwiers MP, Buitelaar JK, Oosterlaan J. Diffusion tensor imaging in attention deficit/hyperactivity disorder: a systematic review and meta-analysis. Neurosci Biobehav Rev 2012;36:1093-106.
45. Abhinav K, Yeh FC, Pathak S, Suski V, Lacomis D, Friedlander RM, Fernandez-Miranda JC. Advanced diffusion MRI fiber tracking in neurosurgical and neurodegenerative disorders and neuroanatomical studies: A review. Biochim Biophys Acta 2014;1842:2286-97.
46. Suri S, Topiwala A, Mackay CE, Ebmeier KP, Filippini N. Using structural and diffusion magnetic resonance imaging to differentiate the dementias. Curr Neurol Neurosci Rep 2014;14:475.
47. Van Essen DC, Ugurbil K, Auerbach E, Barch D, Behrens TE, Bucholz R, Chang A, Chen L, Corbetta M, Curtiss SW, Della Penna S, Feinberg D, Glasser MF, Harel N, Heath AC, Larson-Prior L, Marcus D, Michalareas G, Moeller S, Oostenveld R, Petersen SE, Prior F, Schlaggar BL, Smith SM, Snyder AZ, Xu J, Yacoub E; WU-Minn HCP Consortium. The Human Connectome Project: a data acquisition perspective. Neuroimage 2012;62:2222-31.
48. Craddock RC, Jbabdi S, Yan CG, Vogelstein JT, Castellanos FX, Di Martino A, Kelly C, Heberlein K, Colcombe S, Milham MP. Imaging human connectomes at the macroscale. Nat Methods 2013;10:524-39.
49. Yamada I, Aung W, Himeno Y, Nakagawa T, Shibuya H. Diffusion coefficients in abdominal organs and hepatic lesions: evaluation with intravoxel incoherent motion echo-planar MR imaging. Radiology 1999;210:617-23.
50. Koh DM, Collins DJ. Diffusion-weighted MRI in the body: applications and challenges in oncology. AJR Am J Roentgenol 2007;188:1622-35.
51. Malayeri AA, El Khouli RH, Zaheer A, Jacobs MA, Corona-Villalobos CP, Kamel IR, Macura KJ. Principles and applications of diffusion-weighted imaging in cancer

 

detection, staging, and treatment follow-up. Radiographics 2011;31:1773-91.
52. Lim HK, Kim JK, Kim KA, Cho KS. Prostate cancer: apparent diffusion coefficient map with T2-weighted images for detection--a multireader study. Radiology 2009;250:145-51.
53. Bozgeyik Z, Onur MR, Poyraz AK. The role of diffusion weighted magnetic resonance imaging in oncologic settings. Quant Imaging Med Surg 2013;3:269-78.
54. Kwee TC, Takahara T, Ochiai R, Nievelstein RA, Luijten PR. Diffusion-weighted whole-body imaging with background body signal suppression (DWIBS): features and potential applications in oncology. Eur Radiol 2008;18:1937-52.
55. Knopp MV, von Tengg-Kobligk H, Choyke PL. Functional magnetic resonance imaging in oncology for diagnosis and therapy monitoring. Mol Cancer Ther 2003;2:419-26.
56. Seitz M, Shukla-Dave A, Bjartell A, Touijer K, Sciarra A, Bastian PJ, Stief C, Hricak H, Graser A. Functional magnetic resonance imaging in prostate cancer. Eur Urol 2009;55:801-14.
57. desouza NM, Reinsberg SA, Scurr ED, Brewster JM, Payne GS. Magnetic resonance imaging in prostate cancer: the value of apparent diffusion coefficients for identifying malignant nodules. Br J Radiol 2007;80:90-5.
58. Miao H, Fukatsu H, Ishigaki T. Prostate cancer detection with 3-T MRI: comparison of diffusion-weighted and T2-weighted imaging. Eur J Radiol 2007;61:297-302.
59. Guo Y, Cai YQ, Cai ZL, Gao YG, An NY, Ma L, Mahankali S, Gao JH. Differentiation of clinically benign and malignant breast lesions using diffusion-weighted imaging. J Magn Reson Imaging 2002;16:172-8.
60. Taouli B, Koh DM. Diffusion-weighted MR imaging of the liver. Radiology 2010;254:47-66.
61. Squillaci E, Manenti G, Di Stefano F, Miano R, Strigari L, Simonetti G. Diffusion-weighted MR imaging in the evaluation of renal tumours. J Exp Clin Cancer Res 2004;23:39-45.
62. Herneth AM, Ringl H, Memarsadeghi M, Fueger B, Friedrich KM, Krestan C, Imhof H. Diffusion weighted imaging in osteoradiology. Top Magn Reson Imaging 2007;18:203-12.
63. Ai S, Zhu W, Liu Y, Wang P, Yu Q, Dai K. Combined DCE- and DW-MRI in diagnosis of benign and malignant tumors of the tongue. Front Biosci (Landmark Ed) 2013;18:1098-111.
64. Zhang ZW, Song LJ, Meng QF, Li ZP, Luo BN, Yang YH, Pei Z. High-resolution diffusion-weighted MR imaging of the human lumbosacral plexus and its branches based on a steady-state free precession imaging technique at 3T. AJNR Am J Neuroradiol 2008;29:1092-4.
65. van der Jagt PK, Dik P, Froeling M, Kwee TC, Nievelstein RA, ten Haken B, Leemans A. Architectural configuration and microstructural properties of the sacral plexus: a diffusion tensor MRI and fiber tractography study. Neuroimage 2012;62:1792-9.
66. Tagliafico A, Calabrese M, Puntoni M, Pace D, Baio G, Neumaier CE, Martinoli C. Brachial plexus MR imaging: accuracy and reproducibility of DTI-derived measurements and fibre tractography at 3.0-T. Eur Radiol 2011;21:1764-71.
67. Gasparotti R, Lodoli G, Meoded A, Carletti F, Garozzo D, Ferraresi S. Feasibility of diffusion tensor tractography of brachial plexus injuries at 1.5 T. Invest Radiol 2013;48:104-12.
68. Chuanting L, Qingzheng W, Wenfeng X, Yiyi H, Bin Z. 3.0T MRI tractography of lumbar nerve roots in disc herniation. Acta Radiol 2014;55:969-75.
69. Haakma W, Dik P, ten Haken B, Froeling M, Nievelstein RA, Cuppen I, de Jong TP, Leemans A. Diffusion tensor magnetic resonance imaging and fiber tractography of the sacral plexus in children with spina bifida. J Urol 2014;192:927-33.
70. Scheel M, von Roth P, Winkler T, Arampatzis A, Prokscha T, Hamm B, Diederichs G. Fiber type characterization in skeletal muscle by diffusion tensor imaging. NMR Biomed 2013;26:1220-4.
71. Gaige TA, Benner T, Wang R, Wedeen VJ, Gilbert RJ. Three dimensional myoarchitecture of the human tongue determined in vivo by diffusion tensor imaging with tractography. J Magn Reson Imaging 2007;26:654-61.
72. Gilbert RJ, Napadow VJ. Three-dimensional muscular architecture of the human tongue determined in vivo with diffusion tensor magnetic resonance imaging. Dysphagia 2005;20:1-7.
73. Zijta FM, Froeling M, van der Paardt MP, Lakeman MM, Bipat S, van Swijndregt AD, Strijkers GJ, Nederveen AJ, Stoker J. Feasibility of diffusion tensor imaging (DTI) with fibre tractography of the normal female pelvic floor. Eur Radiol 2011;21:1243-9.
74. Zijta FM, Lakeman MM, Froeling M, van der Paardt MP, Borstlap CS, Bipat S, Montauban van Swijndregt AD, Strijkers GJ, Roovers JP, Nederveen AJ, Stoker J. Evaluation of the female pelvic floor in pelvic organ prolapse using 3.0-Tesla diffusion tensor imaging and fibre tractography. Eur Radiol 2012;22:2806-13.

 

75. Zijta FM, Froeling M, Nederveen AJ, Stoker J. Diffusion tensor imaging and fiber tractography for the visualization of the female pelvic floor. Clin Anat 2013;26:110-4.
76. Kermarrec E, Budzik JF, Khalil C, Le Thuc V, Hancart-Destee C, Cotten A. In vivo diffusion tensor imaging and tractography of human thigh muscles in healthy subjects. AJR Am J Roentgenol 2010;195:W352-6.
77. Kan JH, Heemskerk AM, Ding Z, Gregory A, Mencio G, Spindler K, Damon BM. DTI-based muscle fiber tracking of the quadriceps mechanism in lateral patellar dislocation. J Magn Reson Imaging 2009;29:663-70.
78. Sinha U, Sinha S, Hodgson JA, Edgerton RV. Human soleus muscle architecture at different ankle joint angles from magnetic resonance diffusion tensor imaging. J Appl Physiol (1985) 2011;110:807-19.
79. Schoth F, Burgel U, Dorsch R, Reinges MH, Krings T. Diffusion tensor imaging in acquired blind humans. Neurosci Lett 2006;398:178-82.
80. Hidalgo-Tobon SS. Theory of gradient coil design methods for magnetic resonance imaging. Concept Magn Reson A 2010;36A:223-42.
81. Graessner J. Frequently Asked Questions: Diffusion-Weighted Imaging (DWI). MAGNETON Flash, 2011.
82. Scherrer B, Gholipour A, Warfield SK. Super-resolution reconstruction to increase the spatial resolution of diffusion weighted images from orthogonal anisotropic acquisitions. Med Image Anal 2012;16:1465-76.
83. Stafford RJ. High Field MRI: Technology, Applications, Safety, and Limitations. American Association of Physicists in Medicine (AAPM); 2005. [abstract].
84. Le Bihan D, Poupon C, Amadon A, Lethimonnier F. Artifacts and pitfalls in diffusion MRI. J Magn Reson Imaging 2006;24:478-88.
85. Poot DH, Jeurissen B, Bastiaensen Y, Veraart J, Van Hecke W, Parizel PM, Sijbers J. Super-resolution for multislice diffusion tensor imaging. Magn Reson Med 2013;69:103-13.
86. Mulkern RV, Gudbjartsson H, Westin CF, Zengingonul HP, Gartner W, Guttmann CR, Robertson RL, Kyriakos W, Schwartz R, Holtzman D, Jolesz FA, Maier SE. Multi-component apparent diffusion coefficients in human brain. NMR Biomed 1999;12:51-62.
87. Polders DL, Leemans A, Hendrikse J, Donahue MJ, Luijten PR, Hoogduin JM. Signal to noise ratio and uncertainty in diffusion tensor imaging at 1.5, 3.0, and 7.0 Tesla. J Magn Reson Imaging 2011;33:1456-63.
88. Moser E, Stahlberg F, Ladd ME, Trattnig S. 7-T MR--from research to clinical applications? NMR Biomed 2012;25:695-716.
89. Mukherjee P, Chung SW, Berman JI, Hess CP, Henry RG. Diffusion tensor MR imaging and fiber tractography: technical considerations. AJNR Am J Neuroradiol 2008;29:843-52.
90. Mürtz P, Flacke S, Träber F, van den Brink JS, Gieseke J, Schild HH. Abdomen: diffusion-weighted MR imaging with pulse-triggered single-shot sequences. Radiology 2002;224:258-64.
91. Brockstedt S, Borg M, Geijer B, Wirestam R, Thomsen C, Holtås S, Ståhlberg F. Triggering in quantitative diffusion imaging with single-shot EPI. Acta Radiol 1999;40:263-9.
92. Kwee TC, Takahara T, Koh DM, Nievelstein RA, Luijten PR. Comparison and reproducibility of ADC measurements in breathhold, respiratory triggered, and free-breathing diffusion-weighted MR imaging of the liver. J Magn Reson Imaging 2008;28:1141-8.
93. Chen X, Qin L, Pan D, Huang Y, Yan L, Wang G, Liu Y, Liang C, Liu Z. Liver diffusion-weighted MR imaging: reproducibility comparison of ADC measurements obtained with multiple breath-hold, free-breathing, respiratory-triggered, and navigator-triggered techniques. Radiology 2014;271:113-25.
94. Porter DA, Heidemann RM. High resolution diffusion-weighted imaging using readout-segmented echo-planar imaging, parallel imaging and a two-dimensional navigator-based reacquisition. Magn Reson Med 2009;62:468-75.
95. Porter D, Mueller E. Multi-shot diffusion-weighted EPI with readout mosaic segmentation and 2D navigator correction. Proceedings of the 11th Annual Meeting of the ISMRM; Kyoto, Japan. 2004. (Abstract 442).
96. Griswold MA, Jakob PM, Heidemann RM, Nittka M, Jellus V, Wang J, Kiefer B, Haase A. Generalized autocalibrating partially parallel acquisitions (GRAPPA). Magn Reson Med 2002;47:1202-10.
97. Pruessmann KP, Weiger M, Scheidegger MB, Boesiger P. SENSE: sensitivity encoding for fast MRI. Magn Reson Med 1999;42:952-62.
98. Skare S, Newbould RD, Clayton DB, Albers GW, Nagle S, Bammer R. Clinical multishot DW-EPI through parallel imaging with considerations of susceptibility, motion, and noise. Magn Reson Med 2007;57:881-90.
99. Buxton RB. The diffusion sensitivity of fast steady-state free precession imaging. Magn Reson Med 1993;29:235-43.
100. Jezzard P, Barnett AS, Pierpaoli C. Characterization of and correction for eddy current artifacts in echo planar diffusion imaging. Magn Reson Med 1998;39:801-12.
101. Papadakis NG, Martin KM, Pickard JD, Hall LD,

 

Carpenter TA, Huang CL. Gradient preemphasis calibration in diffusion-weighted echo-planar imaging. Magn Reson Med 2000;44:616-24.
102. Schmithorst VJ, Dardzinski BJ. Automatic gradient preemphasis adjustment: a 15-minute journey to improved diffusion-weighted echo-planar imaging. Magn Reson Med 2002;47:208-12.
103. Alexander AL, Tsuruda JS, Parker DL. Elimination of eddy current artifacts in diffusion-weighted echo-planar images: the use of bipolar gradients. Magn Reson Med 1997;38:1016-21.
104. Koh DM, Blackledge M, Padhani AR, Takahara T, Kwee TC, Leach MO, Collins DJ. Whole-body diffusion-weighted MRI: tips, tricks, and pitfalls. AJR Am J Roentgenol 2012;199:252-62.
105. Xing D, Papadakis NG, Huang CL, Lee VM, Carpenter TA, Hall LD. Optimised diffusion-weighting for measurement of apparent diffusion coefficient (ADC) in human brain. Magn Reson Imaging 1997;15:771-84.
106. Xu C, Sun S. New forms of superparamagnetic nanoparticles for biomedical applications. Adv Drug Deliv Rev 2013;65:732-43.
107. Thoeny HC, Triantafyllou M, Birkhaeuser FD, Froehlich JM, Tshering DW, Binser T, Fleischmann A, Vermathen P, Studer UE. Combined ultrasmall superparamagnetic particles of iron oxide-enhanced and diffusion-weighted magnetic resonance imaging reliably detect pelvic lymph node metastases in normal-sized nodes of bladder and prostate cancer patients. Eur Urol 2009;55:761-9.
108. Birkhäuser FD, Studer UE, Froehlich JM, Triantafyllou M, Bains LJ, Petralia G, Vermathen P, Fleischmann A, Thoeny HC. Combined ultrasmall superparamagnetic particles of iron oxide-enhanced and diffusion-weighted magnetic resonance imaging facilitates detection of metastases in normal-sized pelvic lymph nodes of patients with bladder and prostate cancer. Eur Urol 2013;64:953-60.
109. Hudgins PA, Anzai Y, Morris MR, Lucas MA. Ferumoxtran-10, a superparamagnetic iron oxide as a magnetic resonance enhancement agent for imaging lymph nodes: a phase 2 dose study. AJNR Am J Neuroradiol 2002;23:649-56.
110. Jezzard P, Balaban RS. Correction for geometric distortion in echo planar images from B0 field variations. Magn Reson Med 1995;34:65-73.
111. Patel V, Mistree K. A Review on Different Image Interpolation Techniques for Image Enhancement. IJETAE 2013;3:129-33.
112. Thévenaz P, Blu T, Unser M. Image interpolation and resampling. In: Bankman IN. eds. Handbook of medical imaging, processing and analysis. Orlando: Academic Press, 2000;393-420.
113. Lehmann TM, Gönner C, Spitzer K. Survey: interpolation methods in medical image processing. IEEE Trans Med Imaging 1999;18:1049-75.
114. Borman S, Stevenson RL. Super-resolution from image sequences-a review. In: Circuits and Systems, 1998. Proceedings. 1998 Midwest Symposium on. Notre Dame: IEEE, 1998;374-8.
115. Nedjati-Gilani S, Alexander DC, Parker GJ. Regularized super-resolution for diffusion MRI. In: Biomedical Imaging: From Nano to Macro, 2008. ISBI 2008. 5th IEEE International Symposium on. Paris: IEEE, 2008;875-8.
116. Coupé P, Manjón JV, Chamberland M, Descoteaux M, Hiba B. Collaborative patch-based super-resolution for diffusion-weighted images. Neuroimage 2013;83:245-61.
117. Gupta V. Ayache N, Pennec X. Improving DTI Resolution from a Single Clinical Acquisition: A Statistical Approach Using Spatial Prior. In: Mori K, Sakuma I, Sato Y, Barillot C, Navab N. eds. Medical Image Computing and Computer-Assisted Intervention – MICCAI 2013. Berlin: Springer Berlin Heidelberg, 2013;477-83.
118. Tobisch A, Neher PF, Rowe MC, Maier-Hein KH, Zhang H. Model-Based Super-Resolution of Diffusion MRI. In: Schultz T, Nedjati-Gilani G, Venkataraman A, O'Donnell L, Panagiotaki E. eds. Computational Diffusion MRI and Brain Connectivity. New York: Springer International Publishing, 2014;25-34.
119. Tamada T, Sone T, Jo Y, Yamamoto A, Yamashita T, Egashira N, Imai S, Fukunaga M. Prostate cancer: relationships between postbiopsy hemorrhage and tumor detectability at MR diagnosis. Radiology 2008;248:531-9.
120. deSouza NM, Riches SF, Vanas NJ, Morgan VA, Ashley SA, Fisher C, Payne GS, Parker C. Diffusion-weighted magnetic resonance imaging: a potential non-invasive marker of tumour aggressiveness in localized prostate cancer. Clin Radiol 2008;63:774-82.
121. Chen J, Daniel BL, Diederich CJ, Bouley DM, van den Bosch MA, Kinsey AM, Sommer G, Pauly KB. Monitoring prostate thermal therapy with diffusion-weighted MRI. Magn Reson Med 2008;59:1365-72.

**Cite this article as:** Chilla GS, Tan CH, Xu C, Poh CL. Diffusion weighted magnetic resonance imaging and its recent trend—a survey. Quant Imaging Med Surg 2015;5(3):407-422. doi: 10.3978/j.issn.2223-4292.2015.03.01

 